Molecular Dynamics Simulation of Spontaneous Membrane Fusion during a Cubic-Hexagonal Phase Transition

Siewert-Jan Marrink* and D. Peter Tieleman†

*Department of Biophysical Chemistry, University of Groningen, 9747 AG Groningen, The Netherlands; †Department of Biological Sciences, University of Calgary, Calgary, Alberta T2N 1N4, Canada

ABSTRACT We report a molecular dynamics simulation of the phase transition of monoolein from an inverted cubic phase to an inverted hexagonal phase. The transition proceeds via an intermediate structure consisting of water channels in a cubic geometry, in agreement with the predictions of the modified stalk theory (Siegel, 1999). Two mechanisms are identified by which the topology changes during the transition. Bilayer fusion proceeds via the formation of trans-monolayer contacts, whereas bilayer rupture is observed as a gradual thinning of each monolayer.

INTRODUCTION

Biological membranes consist of a mixture of lipids and proteins organized in a lipid bilayer structure. They contain significant amounts of lipids that do not form bilayers when purified but instead adopt a wide range of morphologies (Yeagle, 1991), including cubic and hexagonal. Nonlamellar lipid phases play several important roles in cell physiology, including in cell-cell adhesion, in mitochondria, and in membrane fusion (Luzzati, 1997). Membrane fusion is required for a variety of essential cell functions as well as viral infections. Because it is difficult to obtain detailed experimental structural data on nonbilayer phases and on intermediate structures in the cell fusion process, much work in this area has been theoretical. Continuum mechanics models have been used extensively to estimate free energies of different proposed intermediates (Siegel, 1999; Kozlovsky and Kozlov, 2002; Lentz et al., 2002; Markin and Albanesi, 2002; Kuzmin et al., 2001). These models have shown the close relationship between lipid phase transitions involving nonlamellar phases and membrane fusion. Recently we described the first atomistic molecular dynamics (MD) simulations of an inverted cubic phase (Q_{II}) of the diamond type of monoolein (GMO) at a variety of state conditions (Marrink and Tieleman, 2001). One of these simulations of a diamond cubic phase showed a complete phase transition to an inverted hexagonal phase (H_{II}). The details of this amazing transition are reported in this paper. The $Q_{II} \rightarrow H_{II}$ phase transition is especially interesting at it is conjectured to proceed via the modified stalk mechanism (MST) (Siegel, 1999). MST predicts intermediate structures similar to the ones that appear during membrane fusion. MD simulations provide the opportunity to study these complex processes in atomic details.

In the remainder of this paper, we give a brief description of the simulation details and explore the atomic details of the phase transition and the membrane rupture and fusion events that occur during this transition. This is followed by a discussion of the limitations and biophysical interpretation of the simulation results.

METHODS

Simulation details

A detailed description about the nontrivial creation of the cubic phase starting structure as well as the simulation details has already been given in a paper describing simulations of just the cubic phase (Marrink and Tieleman, 2001). Briefly, the simulations were performed using the Gromacs software (van der Spoel et al., 1999; Lindahl et al., 2001), at constant temperature (335 K) and isotropic pressure (1 atm) using the weak coupling method (τp = 1.0 ps; τ_T = 0.1 ps) (Berendsen et al., 1984). At these state conditions, GMO experimentally forms a Q_{II} phase of the diamond type (Briggs et al., 1996). The diamond phase of GMO was chosen for its small unit cell (7.4 nm (Briggs et al., 1996)), allowing atomistic MD simulation studies. The system for which the phase transition was simulated is referred to as system I in the original paper (Marrink and Tieleman, 2001). It consists of 504 GMO lipids and 3503 water molecules in a cubic box of size 7.4 nm, modeling one unit cell. Periodic boundary conditions were applied to mimic an infinite system. All atoms are explicitly modeled, except for the hydrogens attached to carbon atoms, for which a united atom model was used. The GMO force field is based on the Gromacs force field, with combined charges from Wilson and Pohorille (1994) and Marrink and Mark (2001). A 1.0-nm cutoff was used for Lennard-Jones interactions, a 1.0/1.5-nm twin range cutoff for Coulomb interactions. All bond lengths and angles involving hydrogen were constrained with LINCS (Hess et al., 1997), which allows a 5-fs integration time step. The initial idealized starting structure was created by evenly covering the smallest symmetry element of the diamond cubic phase with lipids and using symmetry operations to build the whole unit cell. The final starting structure was obtained after an elaborate equilibration procedure (Marrink and Tieleman, 2001) in which the lipid tail groups relax close to the infinite periodic minimal surface that describes the diamond geometry. The results in this paper are based on a subsequent 60-ns unconstrained MD simulation in which the inverted cubic phase spontaneously transforms into an inverted hexagonal phase.

Analysis details

Structural details of the intermediate stages of the transition are characterized by computation of so-called dominant density maps. To construct a

Submitted February 12, 2002, and accepted for publication July 3, 2002.

Address reprint requests to Dr. Peter Tieleman, Department of Biological Sciences, University of Calgary, 2500 University Dr. NW, Calgary, Alberta T2N 1N4, Canada. Tel.: 403-220-2966; Fax: 403-289-9311; E-mail: tieleman@ucalgary.ca.

0006-3495/02/11/2386/07 $2.00

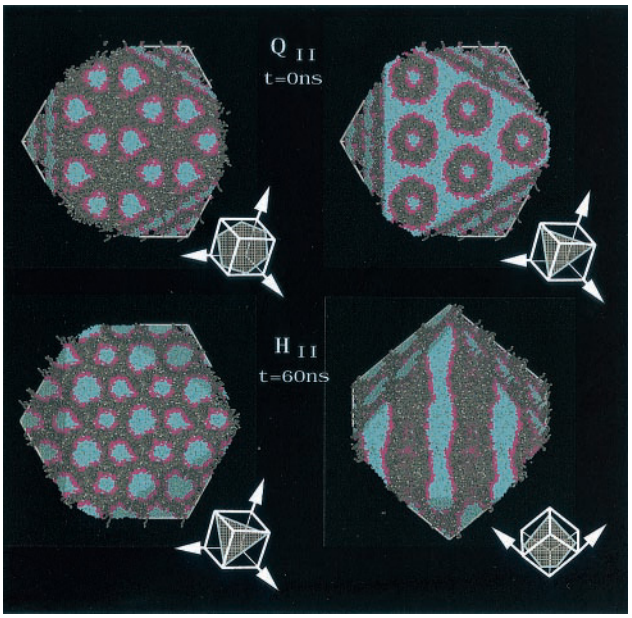

FIGURE 1 Snapshots of the initial diamond Q_{II} (*top*) and final (after 60 ns) H_{II} (*bottom*) system. For each system, two different cross sections are shown (indicated by the *gray planes*) highlighting their structure. The images are constructed from $3 \times 3 \times 3$ simulation cells. Lipid headgroups are purple, lipid tails dark gray, terminal methyl groups light gray, and water molecules blue.

dominant density map, the system is divided into cubic voxels of length 0.3 nm. For each voxel the component with the largest mass density, averaged over 100 ps, is considered dominant. We consider either two components (lipid and water) resulting in binary maps or three components (lipid headgroup, lipid tail, and water) resulting in ternary maps. Thus we obtain a trajectory of smoothed three-dimensional maps, which we use for subsequent structural analysis. A general way of characterizing patterns in statistical physics is by means of the so-called Minkowski functionals, morphological measures describing the topology of the system (i.e., Mecke, 1996). For a three-dimensional system, there are four independent Minkowski functionals: the volume V, the surface area S, the average mean curvature H of the surface, and the Euler characteristic χ. Except for the volume, which remains essentially constant throughout the simulation due to the low compressibility of the system, the other three measures are very sensitive to changes in topology. Using the binary density maps, we defined the surface area as the total connecting area of voxels containing water as the dominant phase bordering voxels containing lipid as the dominant phase. The surface area thus represents the interfacial area between the lipid and aqueous phase. The average mean curvature H and Gaussian curvature K of the interfacial area were obtained from the same maps using the procedure of Hyde et al. (1990). The Euler characteristic is related to the average Gaussian curvature via $\chi = (1/2\pi)\int\int K dS$. χ can take integer values only, and reflects the connectivity of the system.

RESULTS

Starting and final structures

Fig. 1 displays the starting (equilibrated diamond cubic structure) and final structures of our simulation. The inverted diamond phase can be viewed as a multilamellar bilayer system (looking at the sides of the system) with all the lamellae connected to each other by toroidal cross-connections. The inside of a toroidal connection forms a water channel. The three-dimensional structure of the water channels in the inverted diamond phase is that of a diamond network consisting of four tetrahedrally joined water channels per unit cell. A cross section through the water phase separating the lamellae (right view) cuts right through the toroidal cross-connections, resulting in circular bilayers arranged in a triangular pattern. A cross section through one of the lamellae (left view) shows a hexagonal pattern of water channels through the membrane. In the final structure after 60 ns, the GMO lipids have adopted an inverted hexagonal phase. The water forms channels (right view) that are clearly arranged in a hexagonal pattern (left view). As the simulation box remains cubic, the only possible way to obtain a hexagonal symmetry is for the water channel to orient along the cell diagonal, which is what we observe. Note that the channels appear to have an oscillatory shape. This might be an effect of the geometric restraint of a cubic simulation cell.

Intermediate structures

The conversion of the cubic phase into an inverted hexagonal phase is illustrated by Figs. 2–4. Fig. 2 shows the time evolution of the density map of the dominant components of the system, which highlights the redistribution of the three main components (water, lipid headgroups, and lipid tails) inside the system. The stereo views in Fig. 3 of the water phase in each of the intermediate structures reveal the underlying connectivity of the system. Fig. 4 schematically depicts the relocation of the water channels (per unit cell) during the transition. Combined, these figures show that the initial cubic structure is unstable and quickly (1.5 ns) forms additional connections between the bilayers, closing two of the initially four tetrahedrally joined water channels (per unit cell). After 4 ns, a characteristic intermediate structure (I_1) is reached, which consists of a primitive cubic lattice of inverted micelles connected through small connecting water pores in the 110 direction (where 111 corresponds to the direction of the cell diagonal, and 100 to one of the axes). After 8 ns, this intermediate structure converts into another intermediate structure (I_2) by a double reconnecting event: additional water connections are formed between the inverted micelles in the 100 direction, and at the same time the connecting water pores in the 110 direction disappear. The resulting structure consists of water channels oriented along the 100 direction. The channels still exhibit primitive cubic geometry. The I_2 structure appears stable for ~4 ns, but then a slow reorganization occurs in which additional connections in the 011 direction are formed (I_3), which are subsequently replaced by connections in the 111 direction (I_4). Finally (after 40 ns), the 011 connections have disappeared, resulting in the appearance of the H_{II} phase characterized by hexagonally packed water channels running in

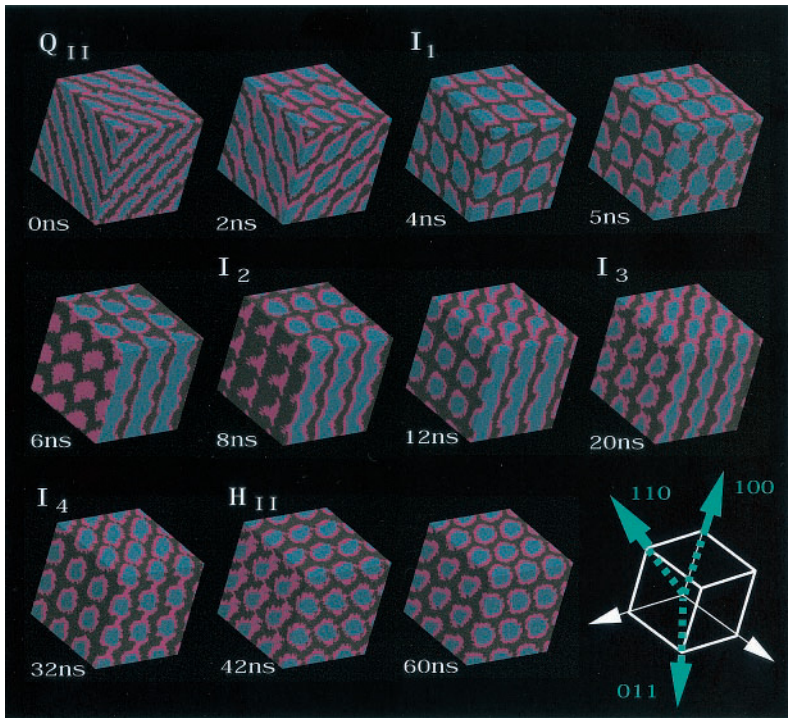

FIGURE 2 Density maps of the $Q_{II} \rightarrow H_{II}$ phase transition showing intermediate structures (I_1–I_4) during the 60-ns simulation. The images are constructed from 3 × 3 × 3 simulation cells. Lipid headgroups are purple, lipid tails dark gray, and water molecules blue. The blue arrows show the directions of the water channels inside the intermediate structures (with the 111 direction perpendicular to the plane of the paper). See text for details.

the 111 direction. This phase remains stable throughout the remaining 20 ns of the simulation.

Minkowski functionals

To further characterize the nature of the transition, Fig. 5 shows the time evolution of the total potential energy ΔH of the system together with the surface area S, the average mean curvature H of the surface, and the Euler characteristic χ: three of the so-called Minkowski functionals, morphological measures that describe the topology of the system (see Methods).

A global comparison of the time dependence of the four curves in Fig. 5 shows that drastic changes appear in all curves at the same time. For instance, the large barrier in potential energy at ~12 ns is accompanied by a large increase in the total interfacial surface area, a clear drop in connectivity (reflected by the Euler characteristic), and a large drop in average mean curvature (implying a surface that is more curved, as the mean curvature for an inverted type phase is negative). These observations reflect the formation of an additional connection between the water channels during the transition from intermediate structure I_2 to I_3. Other significant changes occur when water channels disappear, i.e., at the transition from the cubic structure to the first intermediate structure I_1 around $t = 2$ ns and at the transition from the I_4 intermediate structure to the final H_{II} phase ($t = 40$ ns), or during relocation of the connections (interconversion from I_1 to I_2 at $t = 7$ ns and I_3 to I_4 at $t = 30$ ns). The Euler measure of the final H_{II} as well as of the intermediate structures I_1 and I_2 equals 0, which is characteristic of a structure containing aqueous channels. For the initial cubic structure, the Euler characteristic is −2, the theoretical value for a single unit cell of the diamond phase (Hyde, 1997).

The final hexagonal phase has a potential energy that is only slightly smaller than that of the original cubic phase (~0.5 kT per lipid). Lower energies are actually observed during the transition toward the hexagonal phase, implying that entropy effects play an important role. The interfacial surface area also appears to be a poor judge of the stability of the hexagonal phase. Although the surface area gradually decreases after the hexagonal phase has formed, a lower surface area is observed especially for the I_2 structure. Except for the structure around $t = 12$ ns, which is energetically not favorable, the hexagonal phase, however, has the lowest average mean curvature. Minimization of the average mean curvature thus appears to be an important driving force of the transition.

Membrane fusion and rupture

The observed mechanism of the transition from an inverted cubic to an inverted hexagonal phase is a nice example of the MST (Siegel, 1993, 1999), which describes the intermediates during membrane fusion and lamellar to nonlamellar phase transitions. It is schematically depicted in Fig. 6. It predicts that the transition from Q_{II} to H_{II} proceeds via an intermediate phase that consists of water channels packed in a cubic geometry. This is exactly what we ob-

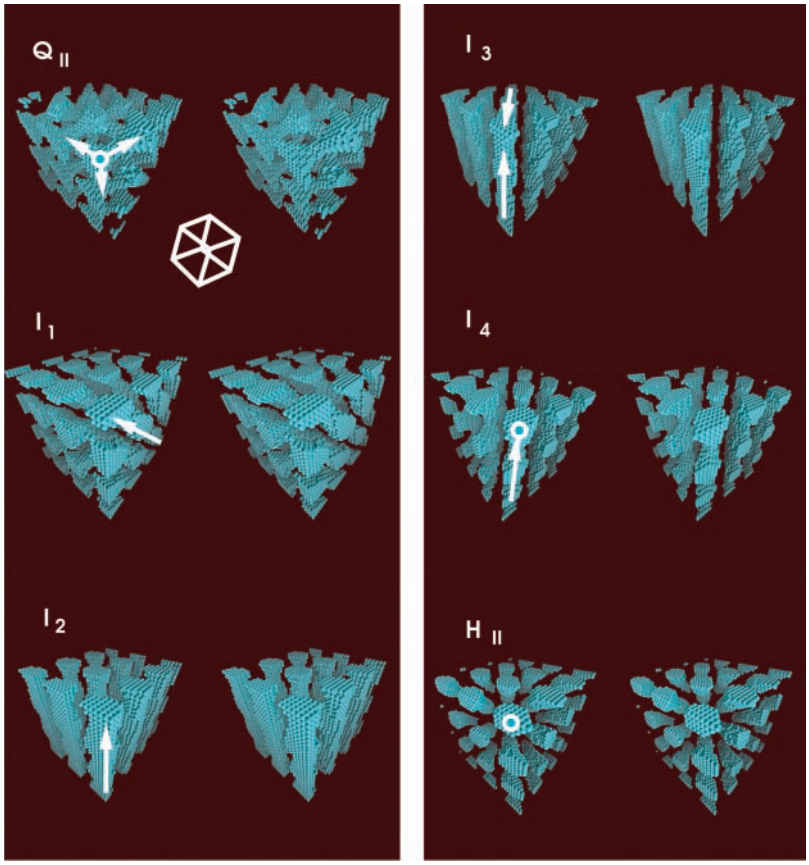

FIGURE 3 Stereo images of the density maps of the intermediate structures. Only the water phase is shown to highlight the structure of the water channels. The images are constructed from $3 \times 3 \times 3$ simulation cells. The system is viewed from the 111 direction as indicated by the white cube. The white arrows denote the direction of the channels. The circles indicate channels running in the 111 direction. See text for details.

serve. Note that the expansion of the intermediate phase directly into a hexagonally packed domain, as predicted by the MST, is not possible in our system due to the geometric constraints of the cubic simulation cell. Instead we observe a series of reconnecting events. According to the MST, the

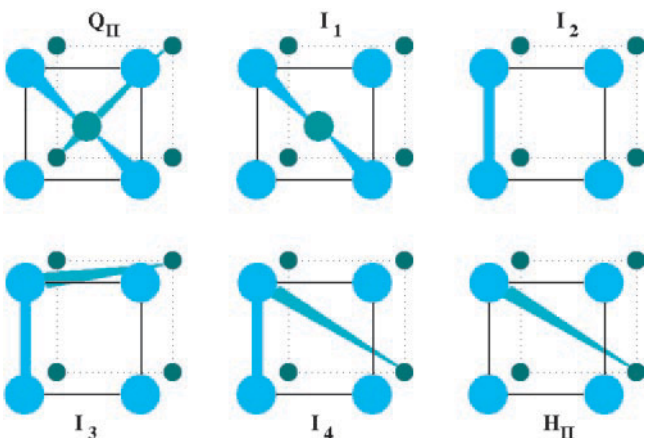

FIGURE 4 Schematic representation of the connectivity of the water channels in the intermediate structures. One simulation cell is shown. The QII phase consists of a diamond network of water channels. Two of these disappear resulting in the I1 structure with connectivity in the 110 direction only. These are replaced by connections in the 100 direction (I2). Additional connections in the 011 direction (I3) are replaced by connections in the 111 directions (I4). Ultimately, the 100 connections disappear resulting in the final H_{II} phase. See text for details.

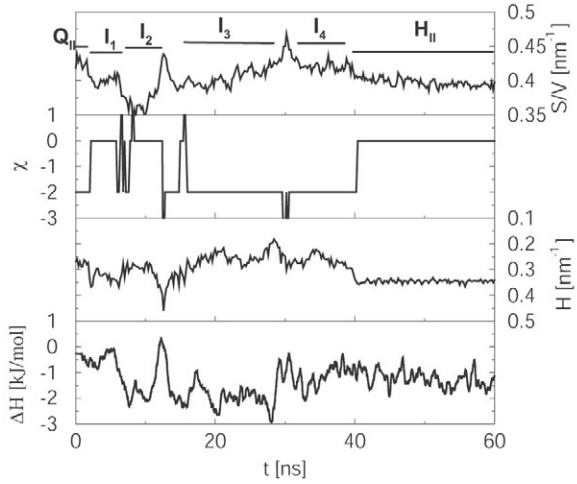

FIGURE 5 Time dependence of integral measures and system energy during the transition. The graphs, from top to bottom, show the interfacial surface area (expressed as surface to volume ratio S/V), Euler characteristic χ, average mean curvature of interface H, and total potential energy difference ΔH (expressed per lipid, with respect to the initial phase). The appearance and disappearance of starting (Q_{II}), intermediate (I_1–I_4), and final (H_{II}) structures is indicated at the top.

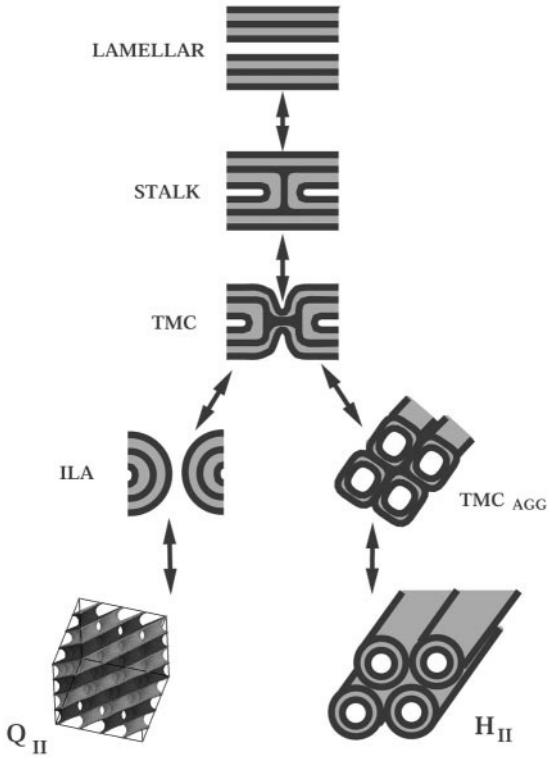

FIGURE 6 Schematic model of the MST, adapted from Siegel (1999). The model describes the transition from lamellar to (inverted) cubic and hexagonal phases. The first step is the formation of a so-called stalk as a result of the fusion between monolayers of separate bilayers. The next step is the formation of a TMC between the outermost monolayers. This intermediate structure can either form a pore or an ILA, which is a precursor to the Q_{II} phase, or it can aggregate with other TMCs to from a precursor phase (TMC_{AGG}) of the H_{II} phase. All the transitions are presumed to be reversible and can be used to predict the phase transition between the Q_{II} and H_{II} phases. Starting from the Q_{II} phase, the ILAs that build the cubic structure merge to form TMCs, which can rearrange to form the TMC_{AGG} phase of cubic symmetry. This phase can subsequently rearrange into the H_{II} phase.

first step in the destabilization of the cubic phase is the closing of the toroidal channels that build the cubic phase (called interlamellar attachments, ILA). The resulting local structures are called trans-monolayer contact (TMC). The left part of Fig. 7 shows a detailed view of the formation of a TMC from an ILA during our simulation. In the initial cubic structure ($t = 0$) the lipids locally form a perfect toroidal channel (or ILA). After 2 ns, this structure has become destabilized. A connection between headgroups of the two opposing bilayers has formed (the term opposing needs to be interpreted with care: the ILA is a three-dimensional structure obtained by rotation around the central axis that runs through the water channel). This connection gradually broadens, but it takes a considerable time before the hydrophobic tails start to connect and a TMC is formed. The initially formed TMC then relaxes to a more stable version. In fact we observe the simultaneous closure

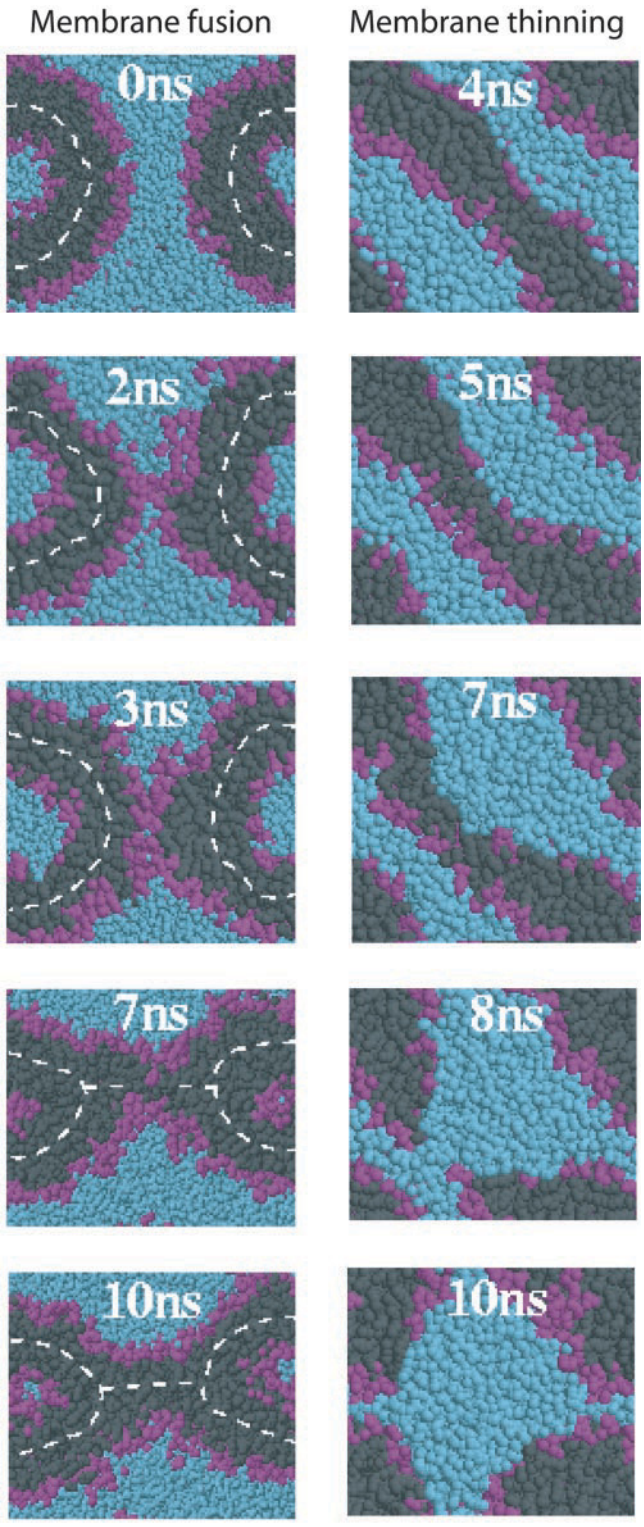

FIGURE 7 Close-up of the formation of a TMC during membrane fusion (*left*) and of the destabilization of a bilayer during a membrane rupture event (*right*). For the coloring scheme, see Fig. 2. White dashed lines indicate the approximate location of the end of a monolayer.

of two of the four tetrahedrally oriented water channels of the original cubic structure. The formation of a TMC appears an essential mechanism to reduce the connectivity of the water phase. TMCs are also observed in the later stages of the simulation whenever water channels disappear. However, during the transition from the intermediate structures toward the final hexagonal phase we have also observed a temporary increase in connectivity (drop of the Euler characteristic in Fig. 5). We find that additional water channels are formed through membrane rupture. The rupture process is illustrated in the right series of snapshots of Fig. 7, which shows the formation of the 100 connection during the transition between intermediate structures I1 and I2. Similar rupture processes are observed during the other connectivity-increasing events in the simulation. We call the mechanism of membrane rupture a thinning mechanism, for essentially what happens is the gradual thinning of a bilayer. At some critical stage, one of the monolayers becomes unstable (5 ns) and eventually completely ruptures (7 ns). The remaining monolayer, now in an energetically very unfavorable state, disappears quickly (after 8 ns). As a result, a connection between previously separated water phases is established (10 ns).

DISCUSSION

The simulated transition of an inverted cubic to an inverted hexagonal phase proceeds via a mechanism strongly resembling the transition mechanism proposed by the modified stalk theory. Our results provide useful insights into the driving forces of the transition and of the structures of the intermediate phases. We showed, with full atomic detail, the closing of water channels to form transmembrane connections as the first step of the phase transition and the appearance of a structure containing water channels in cubic symmetry as an intermediate phase. An important driving force of the transition appears to be the minimization of the mean average curvature of the interface.

Recent continuum calculations suggest that stalk intermediates can have a negligible free energy difference from a bilayer given a suitable geometry (Markin and Albanesi, 2002), which resolves a long-time difficulty with stalk models that assumed an ideal fixed geometry, thus leading to very high free energies. The simulation in this paper, several limitations notwithstanding, suggests an even more disordered stalk and is unable to distinguish between different suggested idealized shapes (Kozlovsky and Kozlov, 2002; Markin and Albanesi, 2002). The fact that this structure is observed at all in a nanosecond time scale simulation suggests its free energy of formation cannot be too high. The second major energetic cost of forming a stalk is the voids that arise when three monolayers come together (Fig. 7) with regularly ordered lipids. It has been suggested that these voids can be filled by hydrophobic solutes in membranes (Markin and Albanesi, 2002). Alternatively, lipid tilting has been suggested as a mechanism to remove these voids (Kozlovsky and Kozlov, 2002; Kuzmin et al., 2001). In the case of GMO lipids in the simulation, it appears the lipids tails are flexible enough to perform this part, as we observe no free space where the monolayers connect.

In our simulations we also observed the rupture of membranes, allowing the establishment of additional water connections. Experimentally, membrane rupture can be induced by applying a lateral membrane stress (using hypoosmotic solutions (e.g., Ertel et al., 1993) or electric fields (e.g., Glaser et al., 1988)). Computational modeling of bilayers under lateral stress (Marrink and Mark, 2001; Groot and Rabone, 2001) show that the bilayer area expands (and the thickness decreases) and, beyond a critical threshold, the bilayer ruptures. The process of membrane rupture as observed in our simulations resembles this mechanism: gradual thinning of the bilayer followed by quick rupture. It seems probable that the required local stress on the membrane is provided by the reorganization of the global structure during the phase transition.

One interesting question is why the simulated cubic structure was unstable in the first place. There are several plausible explanations. First, the cubic diamond phase is found in a narrow temperature/composition range and is known to be only marginally stable: the enthalpy change of the $Q_{II} \rightarrow H_{II}$ transition is $\sim$1 kJ/mol (Hyde et al., 1984). The H_{II} phase is also found experimentally for GMO (Briggs et al., 1996) but at elevated temperatures ($\sim$365 K). The MD force field is possibly not accurate enough to reproduce the phase diagram to such an extent. Second, the cubic phase in the simulation is unable to adjust its surface area by changing the relative lateral and perpendicular cell dimensions (as in lamellar systems), because the phase is isotropic. The experimental uncertainty in unit cell size and composition therefore could cause a significant strain in any particular chosen setup. We have tried a variety of other setups (Marrink and Tieleman, 2001), including slight variations in composition, temperature, and simulation procedure such as the use of a longer cutoff range for the electrostatic interactions. None of these resulted in a stable cubic phase, however. In all cases, destabilization of the Q_{II} phase led to formation of the I1 intermediate structure within 5 ns after release of the constraints. One other simulation was continued for another 10 ns (referred to as system II (Marrink and Tieleman, 2001)). Similarly to the transition observed for system I described in this paper, it reached the intermediate state I3. Therefore, it appears that the general mechanism of the transition is not too critically dependent on the exact state conditions. The initial cubic phase being unstable, however, it is not a transition between thermodynamic states. The simulated phase transition nevertheless is physical, independent of the conditions that caused the destabilization of the starting phase. Experimentally, one could trigger the corresponding transition by an abrupt increase in temperature, for instance. Although the intermediate struc-

tures are relevant, the time scales involved should be interpreted with care. Phase transitions are cooperative phenomena over significant length scales, but because we simulate only one unit cell, cooperativity is likely to be enhanced, making the events fast in comparison with truly macroscopic systems.

CONCLUSION

We observed a phase transition from the diamond cubic phase to the inverted hexagonal phase of monoolein in a 60-ns MD simulation, with intermediates corresponding to those predicted by the modified stalk theory. During this transition, membrane fusion was observed, providing a glance in atomic detail at the fusion mechanism of a simple bilayer. In the fusion intermediates, no voids were observed where the fusing monolayers meet. An additional mechanism was identified, coined thinning mechanism, that allows the establishment of additional water connections through membrane rupture.

We thank Steve Hyde for helpful discussions.

D.P.T. is a Scholar of the Alberta Heritage Foundation for Medical Research and acknowledges support from the Natural Sciences and Engineering Research Council of Canada; S.J.M. is funded by the Royal Netherlands Academy of Arts and Sciences.

REFERENCES

Berendsen, H. J. C., J. P. M. Postma, W. F. van Gunsteren, A. DiNola, and J. R. Haak. 1984. Molecular dynamics with coupling to an external bath. *J. Chem. Phys.* 81:3684–3690.

Briggs, J., H. Chung, and M. Caffrey. 1996. The temperature-composition phase diagram and mesophase structure characterization of the monoolein/water system. *J. Phys. II.* 6:723–751.

Ertel, A., G. Marangoni, J. Marsh, F. R. Hallett, and J. M. Wood. 1993. Mechanical properties of vesicles. I. Coordinated analysis of osmotic swelling and lysis. *Biophys. J.* 64:426–434.

Glaser, R. W., S. L. Leikin, L. V. Chernomordik, V. F. Pastushenko, and A. I. Sokirko. 1988. Reversible electrical breakdown of lipid bilayers: formation and evolution of pores. *Biochim. Biophys. Acta.* 940:275–287.

Groot, R. D., and K. L. Rabone. 2001. Mesoscopic simulation of cell membrane damage, morphology change and rupture by nonionic surfactants. *Biophys. J.* 81:725–736.

Hess, B., H. Bekker, H. J. C. Berendsen, and J. G. E. M. Fraaije. 1997. LINCS: a linear constraint solver for molecular simulations. *J. Comp. Chem.* 18:1463–1472.

Hyde, S. T. 1997. Swelling and structure: analysis of the topology and geometry of lamellar and sponge lyotropic mesophases. *Langmuir.* 13: 842–851.

Hyde, S. T., S. Andersson, B. Ericsson, and K. Larsson. 1984. A cubic structure consisting of a lipid bilayer forming an infinite periodic minimum surface of the gyroid type in the glycerolmonooleate-water system. *Z. Kristallogr.* 168:213–219.

Hyde, S. T., I. S. Barnes, and B. W. Ninham. 1990. Curvature energy of surfactant interfaces confined to the plaquettes of a cubic lattice. *Langmuir.* 6:1055–1062.

Kozlovsky, Y., and M. M. Kozlov. 2002. Stalk model of membrane fusion: solution of energy crisis. *Biophys. J.* 82:882–95.

Kuzmin, P. I., J. Zimmerberg, Y. A. Chizmadzhev, and F. S. Cohen. 2001. A quantitative model for membrane fusion based on low-energy intermediates. *Proc. Natl. Acad. Sci. U.S.A.* 98:7235–7240.

Lentz, B. R., D. P. Siegel, and V. Malinin. 2002. Filling potholes on the path to fusion pores. *Biophys. J.* 82:555–557.

Lindahl, E., B. Hess, and D. van der Spoel. 2001. GROMACS 3.0: a package for molecular simulation and trajectory analysis. *J. Mol. Model.* 7:306–317.

Luzzati, V. 1997. Biological significance of lipid polymorphism: the cubic phases. *Curr. Opin. Struct. Biol.* 7:661–668.

Markin, V. S., and J. P. Albanesi. 2002. Membrane fusion: stalk model revisited. *Biophys. J.* 82:693–712.

Marrink, S. J., and A. E. Mark. 2001. Effect of surface tension on undulations in simulated bilayers. *J. Phys. Chem. B.* 105:6122–6127.

Marrink, S. J., and D. P. Tieleman. 2001. Molecular dynamics simulation of a lipid diamond cubic phase. *J. Am. Chem. Soc.* 123:12383–12391.

Mecke, K. R. 1996. Morphological characterization of patterns in reaction-diffusion systems. *Phys. Rev. E.* 53:4794–4800.

Siegel, D. P. 1993. Energetics of intermediates in membrane fusion: comparison of stalk and inverted micellar intermediate mechanisms. *Biophys. J.* 65:2124–2140.

Siegel, D. P. 1999. The modified stalk mechanism of lamellar/inverted phase transitions and its implications for membrane fusion. *Biophys. J.* 76:291–313.

van der Spoel, D., A. R. van Buuren, E. Apol, P. J. Meulenhoff, D. P. Tieleman, A. L. T. M. Sijbers, B. Hess, E. Lindahl, R. van Drunen, and H. J. C. Berendsen. 1999. Gromacs User Manual version 2.0. University of Groningen, Groningen, The Netherlands.

Wilson, M. A., and A. Pohorille. 1994. Molecular dynamics of a water-lipid bilayer interface. *J. Am. Chem. Soc.* 116:1490–1501

Yeagle, P. 1991. The structure of biological membranes, CRC Press, Boca Raton, FL.